

# We are IntechOpen, the world's leading publisher of Open Access books Built by scientists, for scientists

**6,900**

Open access books available

**186,000**

International authors and editors

**200M**

Downloads

**154**

Countries delivered to

**TOP 1%**

most cited scientists

**12.2%**

Contributors from top 500 universities



**WEB OF SCIENCE™**

Selection of our books indexed in the Book Citation Index  
in Web of Science™ Core Collection (BKCI)

Interested in publishing with us?  
Contact [book.department@intechopen.com](mailto:book.department@intechopen.com)

Numbers displayed above are based on latest data collected.

For more information visit [www.intechopen.com](http://www.intechopen.com)



# Dosimetric Characteristics of the Brachytherapy Sources Based on Monte Carlo Method

Mahdi Sadeghi<sup>1</sup>, Pooneh Saidi<sup>2</sup> and Claudio Tenreiro<sup>3</sup>

<sup>1</sup>*Agricultural, Medical and Industrial School, P.O. Box 31485-498, Karaj,*

<sup>2</sup>*Engineering Faculty, Research and Science Campus, Islamic Azad University, Tehran,*

<sup>3</sup>*Department of Energy Science, SungKyunKwan University, 300 Cheoncheon-dong, Suwon,*

<sup>1,2</sup>*Iran*

<sup>3</sup>*Korea*

## 1. Introduction

The term of brachytherapy, also known as “internal radiotherapy, sealed source radiotherapy, curietherapy or endocurietherapy” is from Greek work brachy means short distance and therapy (treatment) and also known as internal radiotherapy or sealed source radiotherapy. Brachytherapy is a special form of radiotherapy where a radioactive source is carefully placed on or inside the area to be treated. Brachytherapy sources are usually encapsulated; they can be used within the body cavities close to the tumor, placed in a lumen of organs, implanted in to the tumor or placed over the tissue to be treated. The main purpose in radiation therapy is controlling disease and reducing side effects. For a good clinical result one must assure the dose concentrate in the tumor mass and surrounding volume which is at risk of the tumor micro-extentions, while minimizing radiation received by the normal tissue. This can be verified by experimental measurement which is the base of Brachytherapy dosimetry. Due to the high dose gradient near the source and low signal to noise ratio at great distances, experimental dosimetry in Brachytherapy is very complicated or even in small distances is impossible. Also the dose variation with angle in  $4\pi$  geometry of the source must be considered, since routine experimental measurement does not represent this. One of the widely used techniques for solving this problem is Monte Carlo simulation of radiation transport. The calculation of dose distributions at small distances and also validation of experimental measurement can be done by one of the powerful codes such as MCNP, BEAM, EGSnrc, PENELOPE, GEANT4, and ETRAN/ITS. One of the important parameters in the calculation process is validation of the Monte Carlo calculations with measurement results.

This chapter starts with an introduction lecture about brachytherapy history and a short review of the different models for sealed Brachytherapy sources. A brief discuss of brachytherapy dosimetry with computer and measurement is provided. In 1995 the American Association of Physicists in Medicine (AAPM) Task Group No. 43 published a protocol including new formalism for brachytherapy dose calculation and updated in 2004 as TG-43U1. The concept of AAPM recommendation and TG 43 formalism are introduced. Application of Monte Carlo in simulation, guideline for Monte Carlo dosimetry, calculation methodology, requirement for simulation and validation of calculation are then outlined. A

short overview of other application of Monte Carlo in brachytherapy such as eye plaque and applicator design, evaluation of treatment planning system calculation is described. Finally an example of Monte Carlo calculations for dosimetric parameters of  $^{103}\text{Pd}$  brachytherapy seed in three geometric models based on different location of beads inside the capsule is provided.

## 2. History

The use of radioactive sources for treatment of cancerous tumours started shortly after the discovery of radium ( $^{226}\text{Ra}$ ) in 1898 by Madame Curie. This was followed in 1901 by Pierre Curie's self exposure experiment. Brachytherapy developed largely through the use of sealed radium and radon sources, but, quantities and forms of radioactivity useful for brachytherapy were not available until 1940s, when civilian applications of nuclear reactors were encouraged. In 1950s Radium-226 tubes with 1 mm Pt filtration remained the dominant intracavitary source through the late 1960s. Due to the revolutionary of all radiotherapy developments like beam therapy and need of experience to position the brachytherapy sources with sufficient accuracy and radiation exposure hazards for personnel, the role of brachytherapy was not secure in that era. However, over the past three decades, there has been renewed interest in the use of brachytherapy for a number of reasons. The discovery of man-made radioisotopes and remote afterloading techniques has reduced radiation exposure hazards. Newer imaging techniques (CT scan, magnetic resonance imaging, ultrasound) and computerized treatment planning has helped to achieve good clinical outcomes. The advantages of brachytherapy to surgery are treatment simplicity, minimum damage to the surrounding normal tissues and the reduction of side effects for patient after treatment. The advantages of brachytherapy to tele-therapy are its ability in radiation localization on tumor tissue, minimizing radiation to the surrounding normal tissues and rapid dose reduction in normal tissues surrounding the tumor (Ataeinia et al., 2009).

$^{226}\text{Ra}$  sealed in platinum tubes or needles, was the first radionuclide used in brachytherapy treatments. Radium has the advantage of a very long half-life (1620 years), but it also has the disadvantage of producing the alpha-emitting gaseous daughter product radon.  $^{222}\text{Rn}$ , the daughter product of  $^{226}\text{Ra}$  has a half-life of 3.83 days, in a gas form was extracted and sealed within a gold seed, was later used for permanent implants. (Baltas et al., 2007). By the early 1950s, both  $^{226}\text{Ra}$  and  $^{222}\text{Rn}$  have been replaced by newly developed isotopes and brachytherapy had become a well-established and mature modality (Williamson, 2006). In 1950s when produced of other nuclides became available, radium and radon replaced with other new produced radionuclides and they are no longer used. Most common brachytherapy sources emit photons; however, in a few specialized situations such as Craniopharyngiomas which are pediatric tumors, accounting for about 6% of all intracranial tumors in children,  $\beta$  emitting sources are used (Sadeghi et al., 2009a). Brachytherapy photon emitter sources are available in various forms (needles, tubes, seeds, wires, pellets) but are generally sealed to provide shielding against the undesired  $\alpha$  and  $\beta$  radiation emitted from the sources and also to prevent leakage. These sources are used in various types of brachytherapy implant. Sources can be place in to the body cavities near to the tumours (intracavitary), trains of sources are loaded within the lumen of organs (interaluminal), sources are implanted within the tumours (interstitial), or a single source is placed into small or large arteries (intravascular). The dose is then delivered continuously,

either over a short period of time (temporary implants) or over the lifetime of the source to a complete decay (permanent implants) (Mayles et al., 2007).

### 3. Sources used in brachytherapy

Depending on the dose rate of the sources at the dose specification point, brachytherapy treatment classified in three categories: high dose rate sources (HDR) >12 Gy/h, high energy photon emitters such as  $^{137}\text{Cs}$ ,  $^{60}\text{Co}$ ,  $^{192}\text{Ir}$ ,  $^{198}\text{Au}$  are used, medium dose rate (MDR) 2-12 Gy/h, is not common use; and low dose rate sources (LDR), less than 2 Gy/h with low energy photon emitters such as  $^{125}\text{I}$  and  $^{103}\text{Pd}$  (Bethesda, 1985). A brachytherapy source is characterized by the rate at which its strength decays (half-life), by how much radioactivity can be obtained for a given mass of the radioactive source (specific activity), by the energies and types of the radiation particles that are emitted from the source (energy spectrum). These physical brachytherapy source characteristics will guide the clinical utilization. Currently the sources used in brachytherapy categorized in high and low energy sources:

- i. Cesium-137:  $^{137}\text{Cs}$ , a fission by-product, is a popular radium substitute because of its 30-year half-life. It emits  $\beta$ -rays and 0.662 MeV  $\gamma$ -photons.  $^{137}\text{Cs}$  intracavitary tubes are mostly used for intracavitary treatment of gynaecological malignancies. The radioactive material is distributed in insoluble glass micro-spheres. The active source material is then sealed in stainless steel encapsulation cylinders.
- ii. Cobalt-60:  $^{60}\text{Co}$  is produced from thermal neutrons captured by  $^{59}\text{Co}$ . it emits 0.318 MeV  $\beta$ -rays, 1.17 MeV and 1.33 MeV  $\gamma$ -photons and has a half-life of 5.27 years. Cobalt sources are encapsulated with 0.1 to 0.2 mm platinum to filter the  $\beta$ -particles.
- iii. Iridium-192:  $^{192}\text{Ir}$  with a half-life of 73.8 days is the most widely used source for temporary interstitial implants. It emits  $\gamma$ -photons with energies ranging from 9 to 884.5 keV.  $^{192}\text{Ir}$  is used in the form of a wire containing an iridium-platinum radioactive core in a sheath of platinum; and also available in seed format (0.5-mm diameter by 3 mm long) with an active core cylinder contained in stainless steel or platinum encapsulation. The seeds are encapsulated in a 0.8-mm-diameter nylon ribbon and can be used in wire format.
- iv. Gold-198:  $^{198}\text{Au}$  is produced by reactor irradiation of pure gold. Insoluble  $^{198}\text{Au}$  emits  $\beta$ -rays and 412 keV  $\gamma$ -photons; and decays with half-life of 2.7 days. Sources are available for use in intracavitary treatment of the oesophagus in seeds, grains and wires format. Gold-198 seeds are 2.5 mm long and 0.8 mm in outer diameter, and have 0.15-mm-thick platinum encapsulation.

And low energy sources:

- v. Iodine-125:  $^{125}\text{I}$  emits  $\gamma$ -rays and X-rays with energies below 0.0355 MeV and have a half-life of 59.7 days.  $^{125}\text{I}$  sources are packed in a cylindrical encapsulation of titanium shell of 4.5 mm in length and 0.8 mm in diameter, and used mostly for permanent implant treatments of cancers of the prostate, lung, sarcomas, as well as the temporary implant treatment of ocular melanoma when loaded in an eye plaque.
- vi. Palladium-103:  $^{103}\text{Pd}$  is an alternative to  $^{125}\text{I}$  for permanent implants.  $^{103}\text{Pd}$  has lower energy emissions, 20 keV, which allow for a rapid decrease in dose with distance, and also, the short half-life, 17 days, results in higher dose rates and also greater biological effect than  $^{125}\text{I}$ . This radionuclide is available in seed format, encapsulated in titanium tube.

Some physical characteristics of these common brachytherapy sources are summarized in Table 1. (Ling et al., 1995; Nath et al., 2005; Antipas et al., 2001; Wuu & Zaider, 1998).

Isotope	Average photon energy (MeV)	Half-life	Half value layer in lead (mm)	Form of use
<sup>137</sup> Cs	0.662	30 a	6.5	Tube - needle - pellet- seed
<sup>60</sup> Co	1.250	5.26 a	11	Tube- needle- pellet
<sup>192</sup> Ir	0.397	73.8 a	3	Wire - seed
<sup>198</sup> Au	0.412	2.7 d	2.5	Seed
<sup>125</sup> I	0.028	60 d	0.02	Seed
<sup>103</sup> Pd	0.021	17 d	0.01	Seed

Table 1. Some Characteristics of Isotopes Used In Brachytherapy

#### 4. Dose distributions around the sources

Dosimetry, as used in brachytherapy, means the methodology of calculating the dose rate value at an interest point from a source in a given medium. It is important that the physicist know the theoretical basic of dose calculation, manually or using a computer algorithm, around the source in adjacent healthy and critical organs. In modern brachytherapy all available sources have a cylindrical geometry, and are fabricated in core and encapsulation form that can assume a cylindrical symmetry of the dose distribution to their longitudinal axis. The base of brachytherapy dosimetry is experimental measurements and any other theoretical calculations must be validated against measured values. But due to the high dose gradient near the source and low signal to noise ratio at great distances, experimental dosimetry in Brachytherapy is very complicated and in small distances has had a higher degree of uncertainty. Calculation the dose in any points and angles is available by theoretical methods. To improve calculation accuracy it is desirable to make use of Monte Carlo method, which is a computational tool that samples from known probability distributions to determine the average behaviour of a system, it is used in medical physics, particularly in brachytherapy to improve our understanding of all processes associated with radiation emission and transport by using random numbers. So Monte Carlo becomes a powerful tool in medical physics applications (Rogers, 2006; Baltas et al., 2007; Calatayud et al., 2009).

In the Monte Carlo calculations the real source geometry and material is considered; to facilitate the calculations the American Association of Physicists in Medicine (AAPM) Task Group No.43, in 1995 published a protocol (TG-43) introducing a new formalism for dose calculation that the different component of the dose calculation be divided into geometry, attenuation, scattering and anisotropy. This approach is used in modern treatment planning systems and suitable for commissioning. After that in 2004 the AAPM Low-energy Interstitial Brachytherapy Dosimetry subcommittee (LIBD) published an update version of the TG-43 protocol for calculation of dose rate distributions around photon-emitting brachytherapy sources (TG-43U1) (Nath et al., 1995; Rivard et al., 2004).

## 5. The TG-43 formalism

The proposed formula for two-dimensional dose rate is:

$$\dot{D}(r, \theta) = S_K \Lambda \frac{G(r, \theta)}{G(r_0, \theta_0)} g(r) F(r, \theta) \quad (1)$$

Where  $\dot{D}(r, \theta)$  is the dose rate in water at the distance  $r$  in cm from a line source and  $\theta$  denotes the polar angle specifying the point of interest as shown in Figure 1,  $S_K$  is the air-kerma strength has unit of  $U = cGy \text{ cm}^2 \text{ h}^{-1}$ ,  $\Lambda$  is the dose rate constant expressed in  $cGy \text{ h}^{2-1} U^{-1}$ ;  $\frac{G(r, \theta)}{G(r_0, \theta_0)}$  is the geometry factor;  $r_0, \theta_0$  are the reference position,  $r_0 = 1 \text{ cm}$  and  $\theta_0 = 90^\circ$ ,  $g(r)$  is the radial dose function; and  $F(r, \theta)$  is the anisotropy function.

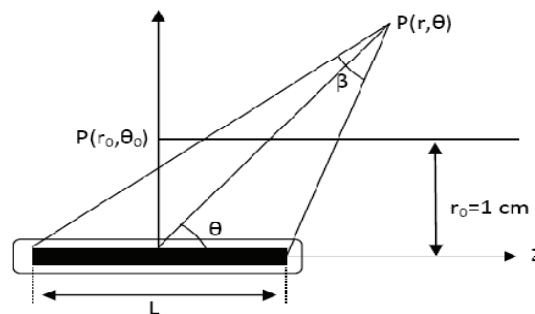


Fig. 1. Coordinate system used for brachytherapy dosimetry calculations.

### 5.1 Brachytherapy source strength

Source-strength designation has gone through several changes over the years. The earliest quantity (mass of radium) was commonly referred to by the unit, milligram radium and still is used in some cases. For sealed sources, especially those of low energy, the encapsulation reduces the air kerma and dose rates below those which would be produced by the bare source. Thus the strength is generally given as apparent activity, which is less than the encapsulated activity. Apparent activity is the activity of a hypothetical point source of the same radionuclide which would produce the same air kerma rate, at the same large distance, as that measured on the transverse axis of a sealed source. The design of the source capsule also influences the dose distribution around the source. It is quite possible for two sources of the same radionuclide and same apparent activity to have different dose distributions. (Nath et al., 1997).

### 5.2 Air-kerma strength, $S_K$

Air-kerma strength is the product of air-kerma rate in free space at the measured distance from the source centre along the perpendicular bisector,  $r$ , multiplied by the square of this distance,  $r^2$ :

$$S_K = \dot{K}_\delta(r)r^2 \quad (2)$$

Distance  $r$  must be chosen large enough, relative to the linear dimension of the source, to find independent air kerma strength of distance.

$\dot{K}_\delta(r)$  is the air kerma rate in vacuo and for the photons of energy greater than a certain cut-off value of  $\delta$  which is typically 5 keV for low-energy photon emitting sources. This value is

dependent on the assumption that photons with energies up to this cut-off value are not tissue penetrating. The qualification "in vacuo" means that the measurements should be corrected for photon attenuation and scattering in air and any other medium interposed between the source and detector.

### 5.3 Dose-rate constant, $\Lambda$

The dose rate constant,  $\Lambda$ , is defined as the dose rate in water at the reference point,  $D(r_0, \theta_0)$ , namely at a distance of  $r_0=1$  cm on the transverse axis ( $\theta=90^\circ$ ), per unit air kerma strength,  $S_K$ , as seen in Equation (3):

$$\Lambda = \frac{D(r_0, \theta_0)}{S_K} \quad (3)$$

The dose rate constant depends on both the radionuclide and source model, and is influenced by both the source design (radioactive distribution and encapsulation) and also the methodology used to determine  $S_K$ .

### 5.4 Geometry function, $G_X(r, \theta)$

The geometry function,  $G_X(r, \theta)$ , takes into account the effect of the distribution of radioactive material inside the capsule on the dose distribution and is a function of both  $r$  and  $\theta$ . physically it provides an effective inverse square-law and neglects scattering and attenuation of emitting photons around the source (Karaiskos et al., 2000). The subscript "X" is to indicate a point-source, "P" or line-source, "L", geometry function. The values of the geometry function can then be calculated as follow:

$$G_P(r, \theta) = r^{-2} \quad \text{For the point-source}$$

$$G_L(r, \theta) = \begin{cases} \frac{\beta}{(r^2 - \frac{L^2}{4})^{-1}} & \text{if } \theta \neq 0^\circ \\ \frac{r \sin \theta}{(r \cos \theta - L/2)} & \text{if } \theta = 0^\circ \end{cases} \quad \text{For the line-source} \quad (4)$$

$$\beta = \tan^{-1}\left(\frac{r \sin \theta}{r \cos \theta - L/2}\right) - \left(\frac{r \sin \theta}{r \cos \theta + L/2}\right)$$

Where  $\beta$  is the angle in radians, subtended by  $P(r, \theta)$  and two ends of active length of the source. In the case where radioactive material is distributed over a cylindrical volume, the active length,  $L$ , will be the length of the cylinder (Fig.1). For brachytherapy sources containing multiple radioactive pellets,  $L$  is given by:

$$L_{eff} = \Delta S \times N \quad (5)$$

Where  $N$  is the number of discrete pellets contained in the source, and  $\Delta S$  is the center to center distance of the pellets. The active length should be less than the length of source capsule. In the case where it is greater, the effective length of the seed is considered the distance between proximal and distal aspects of the activity distribution.

### 5.5 Radial dose function, $g_X(r)$

The radial dose function describes the effect of tissue attenuation on photons emitted from a brachytherapy source and accounts for the dose fall-off along the source transverse axis due to the photon scattering and attenuation. Equation (6) is defined the  $g_X(r)$  as:

$$g_X(r) = \frac{\dot{D}(r, \theta_0) G_X(r_0, \theta_0)}{\dot{D}(r_0, \theta_0) G_X(r, \theta_0)}, \quad X = P \text{ or } L \text{ (Point or line source)} \quad (6)$$

### 5.6 2D anisotropy function, $F(r, \theta)$

The 2D anisotropy function describes the variation of dose in the longitudinal plane of the seed. Variations are due to the distribution of radioactivity within the seed, self-absorption and oblique filtration of the radiation in the encapsulating material.  $F(r, \theta)$  Is obtained by the following formula:

$$F(r, \theta) = \frac{\dot{D}(r, \theta)}{\dot{D}(r, \theta_0)} \frac{G_L(r, \theta_0)}{G_L(r, \theta)} \quad (7)$$

## 6. The use of Monte Carlo to obtain the dosimetric parameter

The most important role of Monte Carlo in brachytherapy is to obtain the dosimetric parameters of the sources with high spatial resolution. As mentioned above, "dosimetry" refers to estimation of absorbed dose by means of experimental or fundamental theoretical techniques about single brachytherapy sources. Due to the high dose gradient near the brachytherapy sources at short distances in water or water-equivalent phantoms, near-field dosimetry of brachytherapy sources is very complicated. To avoid dosimeter averaging effects, very high resolution (les than 0.5 mm) dosimeters are required (Chiu-Tsao et al., 2007; Williamson 1991); also low energy-response of some detectors; and lack of reproducibility, increase the uncertainty in experimental dosimetry.

Monte Carlo simulation is the theoretical method for calculation of dosimetric parameters. Monte Carlo simulation easily can obtain dosimetric parameters at small distances and all angles without any limitation and complication. For low energy photon emitters such as  $^{125}\text{I}$  and  $^{103}\text{Pd}$ , photoelectric absorption contributes a larger proportion of the dose to tissue than for higher energies. Therefore, small variations in tissue atomic number result in significant effects on dose. These effects can also be calculated precisely by Monte Carlo simulation by replacing the different phantom materials in different geometries (Dale et al., 1985; Prasad 1985; Huang 1990).

According to TG-43U1 recommendation, the main guideline items that should be considered in MC simulation for accurate calculations are as follow:

1. The information of source dimension, composition of encapsulation and internal components and their geometry must be specified clearly; typically these data obtained by manufacturer's report and Monte Carlo allows complete flexible description of the real geometry of the sources.
2. Simulation should be performed in a 30 cm water phantom for low energy photon-emitters like  $^{125}\text{I}$  and  $^{103}\text{Pd}$ , and 40 cm water phantom for high energy photon-emitters such as  $^{137}\text{Cs}$  and  $^{192}\text{Ir}$ , to consider all the scattering effects of the surrounding medium.
3. To extract the absorbed dose distribution from the particle transport simulation, one has to define a so-called tally or scoring function. The size and position of scoring voxels

- (detectors) should define in a way to decrease the uncertainty; usually Monte Carlo uses voxels at radial distances up to 10 cm, for low energy sources and to 15 cm for high energy sources, away from the source at different polar angles. The voxel sizes are an important issue in simulation. To minimize the systematic error, the voxel sizes should be small as low as possible.
4. Enough histories should be calculated to ensure that the statistical uncertainties are in confidence range.
  5. The statistical uncertainty should be  $\leq 2\%$  (for  $r < 5$  cm) and  $\leq 1\%$  in  $S_K$  with  $k=1$ .
  6. Due to the lack of old cross-section libraries for low energy photons, modern and new cross-section libraries should be used in Monte Carlo simulation.
  7. Mechanical movement of the internal component of the seeds should be considered in the simulation. Because the location of the sources can vary with seed orientations and can affect on dosimetric parameters.

To calculate the dosimetric parameters, two simulations are needed: one with the source model in the medium which is usually water phantom, to obtain the dose at interest points; second simulation by modelling in vacuum to obtain the air kerma strength and geometry function. For low energy photon emitters such as  $^{125}\text{I}$  and  $^{103}\text{Pd}$ , the source is modelled in a centre of a 30 cm spherical water phantom, large enough to consider effects of the surrounding medium. For HDR sources like  $^{137}\text{Cs}$  and  $^{192}\text{Ir}$ , the photon energies are higher than those emitted by  $^{125}\text{I}$  and  $^{103}\text{Pd}$ , therefore a 40 cm diameter spherical phantom is considered for modelling (Rivard, 2007; Perez-Calatayud et al., 2004; Melhus and Rivard, 2006). Generally for low energy photon emitters,  $S_K$  is calculated in several air-filled detectors at distances ranging from 5 to 150 cm in the transverse plane in free air geometry, which is found to be independent of distance. Due to the low energy of the photons from the low energy sources, it is assumed in the Monte Carlo calculations all electrons generated by the photon collisions are absorbed locally and the electronic equilibrium exists, so dose is equal to kerma at all points of interest [Hosseini et al., 2009 & Sadeghi et al., 2008b].

It should be noted that for high energy sources, electronic equilibrium, and consequently, water kerma dose approximation, may be safely assumed only at distances greater than 1 mm from the sources (Wang & Li 2000, Baltas 2001).

Geometry function just provides the inverse square law correction depending only on the shape of the active core and not on the encapsulation or radionuclide. Thus the medium inside and around the source has been considered as vacuum in order to disregard the absorption and scattering in the seed and the surrounding media. The geometry function value is given by Equation (4). For calculating geometry function, the mass densities of all materials within the entire computational geometry should be set equal to zero so there were no interaction and particles streamed through the seed phantom geometry and it is common to approximate the active source material distribution within a brachytherapy source by an idealized geometry such as a line. (Levitt et al. 2006, Rivard 2001).

To obtain radial dose function values, Monte Carlo method is the best choice. Due to the complication of experimental measurement at small distances, dose rates are estimated down to the smallest distances and experimental values are only consider for validation of the Monte Carlo simulation results. By applying the Equation (6) radial dose function, which is the radial dependence of the dose rate value at the reference polar angle,  $\theta=90^\circ$ , is obtained and equal to unity at distance 1 cm. Dose rates can be estimated by linear interpolation from data tabulated at discrete points. The tabulated values are fit to polynomial which is proposed in TG-43U1.

$$g_X(r) = a_0 + a_1r + a_2r^2 + a_3r^3 + a_4r^4 + a_5r^5 \quad (8)$$

Parameters  $a_0$  to  $a_5$  should be calculated by fifth order polynomial fit to the tabulated  $g_X(r)$  data within  $\pm 2\%$ . Commonly radial distance range for low energy sources is from 0.5 to 7.0 cm and for high energy sources is up to 15.0 cm. Depending on the source encapsulation design, in some cases calculation at distance as low as 0.1 cm could be also needed.

The values of the anisotropy function, defined by Equation (7), can be derived from Monte Carlo calculated at different radial distances from  $r= 0.25$  to 7.0 cm for low energy sources and up to 15.0 cm for high energy sources, and different polar angles from  $\theta=0^\circ$  to  $90^\circ$  for symmetric sources about the transverse plane and from  $\theta=0^\circ$  to  $180^\circ$  for source design that are asymmetric about the transverse plane. According to Equation (7), the anisotropy function value at any radial distance on transfer plan, is always 1.0. Its value off the transfer plan decreases as:  $r$  increases, encapsulation thickness increases,  $\theta$  approaches  $0^\circ$  or  $180^\circ$  and energy of photon decreases (Bethesda et al., 1985).

## 7. Validation of Monte Carlo modelling

As the Monte Carlo method has its own uncertainties, the preferred general approach is to use other determination method, and compare the results. According to TG-43U1 recommendation and other research publications, it has been accepted as a standard method that validation of Monte Carlo calculations via independent studies is required. To verify the Monte Carlo calculations, the experimental data sets should be compared with calculated data. For the experimental dosimetry in brachytherapy it is necessary to introduce a dosimeter in the radiation field of a source which should provide a measurable reading and present an adequate sensitivity with small sensitive volume to avoid dose volume averaging. The dosimetric system that provides optimum compromise between these prerequisites is TL dosimetry TLDs are currently considered as the dosimeter of choice for experimental dosimetry in the entire energy range of brachytherapy sources and TLD dosimetry is an accepted approach to validate the Monte Carlo simulation. Because the value of dosimetric parameters strongly depends on source material, seed model, encapsulation thickness and geometry, the experimental measurement should be done for the same seed which is modeled in Monte Carlo simulation. The steep dose gradient around low energy radio-nuclides such as  $^{125}\text{I}$  and  $^{103}\text{Pd}$  causes significantly dosimetric uncertainty. So the validation should be done for the larger distances, for example 1-5 cm then all other data especially for small distances, can get from Monte Carlo results. For other sources with higher energy like  $^{137}\text{Cs}$  and  $^{192}\text{Ir}$ , the dependence of dosimetric parameters of source geometry and material is low and measured value can obtain from similar source design. If the Monte Carlo and experimental datasets are compatibles within the acceptable uncertainties, a set of consensus value of dosimetric parameters would be established. The consensus data were defined as the ideal candidate dataset having the highest resolution, covering the largest distance range, and having the highest degree of smoothness. The consensus dose rate constant value should be obtained by the averaged experimental and Monte Carlo  $\Lambda$  values:

$$\text{CON}\Lambda = [\text{EXP}\Lambda + \text{MC}\Lambda]/2. \quad (9)$$

Or it should be selected as being representative of the collection of values available in the literature.

The consensus values for anisotropy function and radial dose function for most source models are mostly selected from Monte Carlo results that spanned the required range of radial distances and angles and had sufficiently fine spacing to make the interpolation between points accurate. Also Monte Carlo study considers the beta particles and electrons emitted by the source.

## 8. Other application of Monte Carlo

The Monte Carlo dose calculations are mostly used to obtain the dosimetric parameters around the brachytherapy sources to use in treatment planning systems. Calculated data provide the specific dose distributions based upon the actual locations of the sources in and around the patient; and also as a benchmarking tool for treatment planning systems (Williamson et al., 1999; Anagnostopoulos et al. 2003). The main goal of clinical treatment planning is to find the best way to maximize the tumor dose and minimize the dose to the healthy tissue. Most current commercial treatment planning systems implemented the TG-43 formalism and the recommended dosimetry parameters in their systems to determine the dose distributions. Monte Carlo calculations can obtain the approximations in the calculations done by the treatment planning system. For low-energy sources, a major problem is characterizing tissue heterogeneities, requires estimation of the photoelectric cross section as well as tissue density these can have significant errors near inhomogeneities in the patient. Monte Carlo dose calculations can account for tissue-composition heterogeneities (Chibani and Williamson, 2005; Devic et al. 2000). Monte Carlo dose calculations, when carefully validated against measurements, provide the highest level of accuracy for dose calculation in treatment planning, in situations where measurements are difficult or even impossible. Monte Carlo also can use for study and design of applicators. Intracavitary brachytherapy is mostly used for cancers of the cervix, uterine and vagina. Several rigid applicators have been used for intracavitary brachytherapy but it requires careful design of the applicators and precise placement of the sources with respect to the tumor volume and surrounding organs. The most clinical complication of intracavity brachytherapy in this case results from the high dose delivered to the critical surrounding organs such as bladder and rectum. Because the common types of source for treatment of gynecology are high energy sources,  $^{137}\text{Cs}$  and  $^{192}\text{Ir}$ . Monte Carlo simulation can play an important role to keep the dose to these critical organs as low as possible by obtain the dose rate in interest points.

Another use of Monte Carlo in brachytherapy is its application in design of eye plaque. Radioactive eye plaque therapy is incorporating the use of radioactive seeds in a widely used technique for the treatment of ocular tumors. Monte Carlo simulation is performed to fully model the brachytherapy seeds loaded in the eye plaque to obtain the dose distribution in critical ocular structure and central axis of plaque. Brachytherapy seeds are placed in slots within a polymer carrier, Monte Carlo is possible to obtain the attenuation effect of the plaque backing, most often made of gold or stainless steel, and polymer carrier (Acrylic or Silastic) on dose distribution. Physical characteristics of photons emitted by different seed models (position, energy, location, and direction) are strongly dependent on seed construction, especially since brachytherapy sources are often constructed of high atomic number materials. In some cases, due to the presence of seed carrier inside the plaque the emitted photons from sources attenuate, thus more  $S_K$  per seed is needed to deliver the prescription dose to the tumor volume, that can be obtained by Monte Carlo simulation. For

example Granero et al., 2004 calculated the dose rate around the eye plaque loaded with  $^{125}\text{I}$  sources in Acrylic insert and they found Acrylic insert has no attenuation effect on dose rate and the presence of acrylic insert can be negligible in the calculations. In other Mont Carlo simulations Chiu-Tsao et al., 1993, obtained 10% dose reduction at 1cm for Silastic insert; Thomson et al., 2008 reported 17% dose reduction for  $^{103}\text{Pd}$  seed at distance of 1 cm in eye plaque due to presence of Silastic insert; and also calculated results by (Melhus & Rivard, 2008) demonstrated approximately  $22.6\%\pm0.5\%$ ,  $13.0\%\pm0.3\%$ , and  $10.8\%\pm0.3\%$  more  $S_K$  in each  $^{103}\text{Pd}$ ,  $^{125}\text{I}$ , and  $^{131}\text{Cs}$  seed contained in a eye plaque, respectively was required to deliver the same dose to the apex of tumor.

According to the Monte Carlo calculated data, size, shape and location of the eye tumor, standard eye plaque should design. Iodine-125 is currently the most commonly used source for radioactive eye plaque therapy. Few centers use palladium-103, and available reports indicate that because of its low energy emissions 20 keV which allow for a rapid decrease in dose with distance; and also, the short half-life, 17 days, result in higher dose rates and favorable dose distribution (Finger et al., 1999; Hall et al. 1991; Finger et al., 1991; Sadeghi & Hosseini, 2010). Generally for the Monte Carlo simulation, the eye plaque is centered in a 15 cm radius water phantom to provide adequate photon backscatter and large enough to consider all the scattering effects of the surrounding medium. The Monte Carlo simulations provide the dose in a voxel per history. The dose rate is calculated by dividing this number by the air kerma strength per history for the relevant seed type and multiplying by the number of seeds and the air kerma strength per seed:

$$\dot{d}(x, y, z) = {}_{SP}\dot{d}(x, y, z) \left[ {}_{source}S_K \left( \frac{S_K}{A} \right)^{-1} K \right] \cdot n \quad (10)$$

Where  $\dot{d}(x, y, z)$  is the dose rate at the position  $x, y, z$  to deliver the prescription dose;  ${}_{SP}\dot{d}(x, y, z)$  is the dose rate per starting particle at position  $x, y, z$ ;  ${}_{source}S_K$  is the  $S_K(U)$  per source needed to deliver  $\dot{d}(x, y, z)$ ;  $\frac{S_K}{A}$  is the ratio of the  $S_K(U)$  and activity  $A(\text{mCi})$  for a given source;  $K$  is the photons emitted per unit activity and  $n$  is the number of sources. Finally the total dose is calculated by integration  $\dot{d}(x, y, z)$  over the prescribed treatment time. According to American Brachytherapy Society recommendation for uveal melanoma the prescription treatment time is 3 to 7 consecutive days to deliver a total prescription dose. The prescription dose depends on the prescription point, method of dose prescription and dosimetry calculation assumption but following the Collaborative Ocular Melanoma Study (COMS) group dosimetry calculation assumption, is 85 Gray to the tumor apex (Nag et al., 2003; Baltimore 1995; Melia et al., 2001; Granero et al., 2010). In fact Monte Carlo Calculated dose rate for the eye plaque at interested point in the eye region has helped design of eye plaque as a valuable brachytherapy dosimetry tool.

## 9. Example of Monte Carlo calculations for dosimetric parameters of $^{103}\text{Pd}$ brachytherapy seed

This example presents Monte Carlo (MC) simulation results for the dosimetry parameters of the IR- $^{103}\text{Pd}$  seed (Saidi et al., 2010).

Dose distributions in this example were simulated with the MCNP5 Monte Carlo (MC) radiation transport code published by Los Alamos National Laboratory ([mcnp-green.lanl.gov/index.html](http://mcnp-green.lanl.gov/index.html), 2008) and the MCPLIB04 photon cross-section library is based

on the ENDF/B-VI data (BNL.NCS-17541, 8th ed., 2000). In the calculations, the titanium characteristic X-ray production were suppressed with  $\delta=5$  keV ( $\delta$  is the energy cutoff) (Nath et al., 1995). The spherical water phantom was modeled with a 30 cm diameter with an atomic ratio of 2:1 for H:O and  $\rho=0.998$  g/cm<sup>3</sup>. The seed source placed in the center of the phantom for the calculation of all dosimetric parameters at radial distances of  $r= 0.25, 0.5, 0.75, 1, 2, 3, 4, 5$  and 7 cm, away from the source and at polar angles relative to the seed longitudinal axis from  $0^\circ$  to  $180^\circ$  with  $10^\circ$  increment. To validate the Monte Carlo simulation, results were compared by experimental values (Raisali et al., 2008). The simulations were performed up to  $1.1 \times 10^9$  histories. With this number of histories, statistical uncertainty for the source along the longitudinal axis at  $r \leq 5$  cm is lower than 1.3%, at 7 cm is 4.5% and at other angles it is between 0.04% and 0.1%. In air, with  $1.5 \times 10^8$  histories, statistical uncertainty is 0.1%.

Figure 2(a), shows a schematic diagram of the IR-<sup>103</sup>Pd seed. The seed contains five resin beads, which are packed inside a titanium cylinder of 4.8 mm length, 0.7 and 0.8 mm internal and external diameter respectively, and with an effective length of 3 mm. <sup>103</sup>Pd radioactive material is absorbed uniformly in the resin bead volume. As the beads are free to move within the titanium capsule, their location can vary with seed orientations. Saidi et al. (2010), simulated three geometric models of the seed, ideal, vertical and diagonal, as shown in Figure 2(a), (b) and (c) respectively.

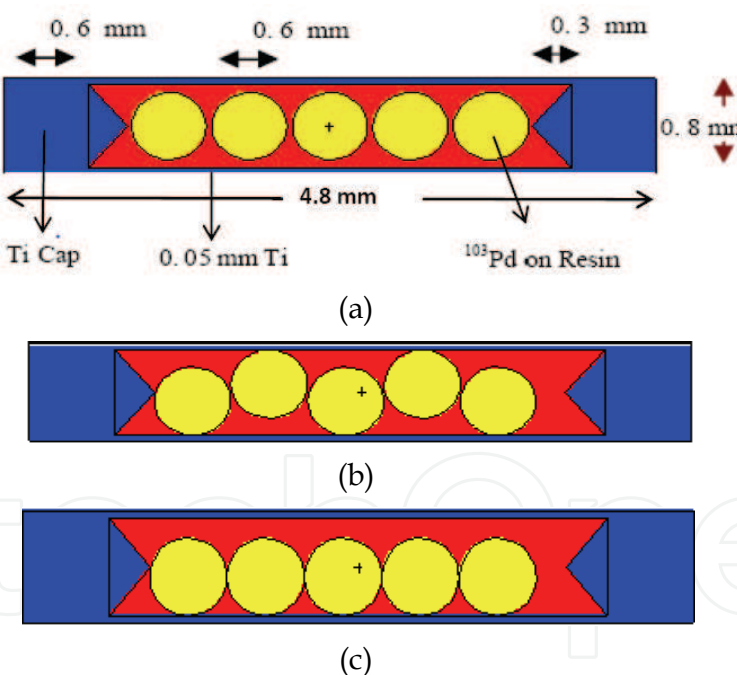


Fig. 2. Schematic diagram of the IR-<sup>103</sup>Pd seed in Monte Carlo calculation for various seed orientations: (a) Ideal orientation, (b) vertical orientation, and (c) diagonal orientation (<sup>103</sup>Pd absorbed in resin).

The dose rate constant for the <sup>103</sup>Pd seed was calculated by using the Equation (3). Due to the low energy of the photons from <sup>103</sup>Pd, it was assumed in the Monte Carlo calculations all electrons generated by the photon collisions are absorbed locally, so dose is equal to kerma at all points of interest (Sadeghi et al., 2008b). The air-kerma rate of the IR-<sup>103</sup>Pd seed in this example was estimated by calculating the dose in 1 mm-thick air-filled rings in a vacuum.

The rings were bounded by  $86^\circ$  and  $94^\circ$  conics and defined with a radial increment of 5 cm to 150 cm along the transverse axis of the source and also the MCNP F6 tally, was used for calculate the dose distribution around the seed in each of the three orientations consider in this work.

Source type	Method	Medium	$\Lambda$ (cGy h <sup>-1</sup> U <sup>-1</sup> )	Reference
IR- <sup>103</sup> Pd	Monte Carlo (vertical)	Liquid water	$0.695 \pm 0.021$	Saidi et al. (2010)
IR- <sup>103</sup> Pd	Monte Carlo (ideal)	Liquid water	$0.716 \pm 0.021$	Saidi et al. (2010)
IR- <sup>103</sup> Pd	Monte Carlo (ideal)	Liquid water	$0.706 \pm 0.001$	Raisali et al. (2008)
New <sup>103</sup> Pd	Monte Carlo (vertical)	Liquid water	$0.673 \pm 0.001$	Rivard et al. (2004b)
New <sup>103</sup> Pd	Monte Carlo (vertical)	Liquid water	$0.675 \pm 0.020$	Saidi et al. (2010)
MED3633	TLD dosimetry	Solid water	$0.688 \pm 0.05$	Wallac & Fan (1999)
	Monte Carlo	Liquid water	$0.677 \pm 0.02$	Li et al. (2000)
Theragenics 200	TLD dosimetry	Solid water	$0.650 \pm 0.08$	Nath et al. (2000)
	Monte Carlo	Liquid water	$0.686 \pm 0.03$	William (2000)

Table 2. Monte Carlo calculated dose rate constant,  $\Lambda$ , of the IR-<sup>103</sup>Pd seed and new <sup>103</sup>Pd source and comparison with the measured and calculated values of model MED3633 and Theragenics200.

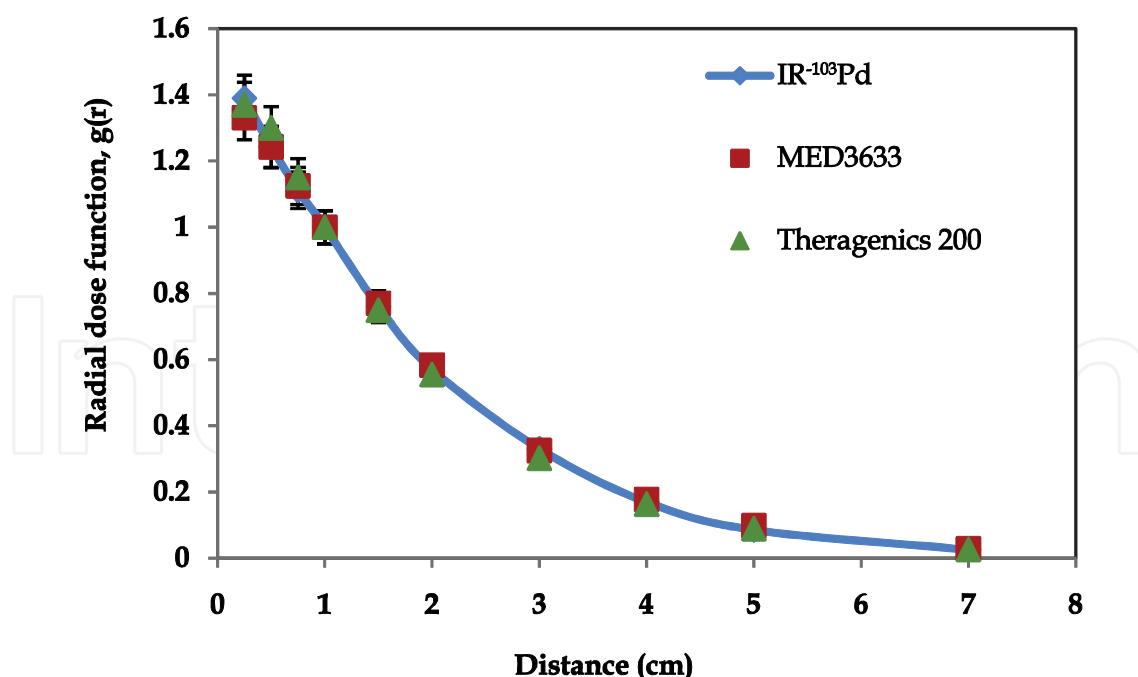


Fig. 3. Comparison of the Monte Carlo calculation radial dose function of IR-<sup>103</sup>Pd (Saidi et al., 2010) seed with the MED3633 and Theragenics model 200 sources (Rivard et al., 2004a).

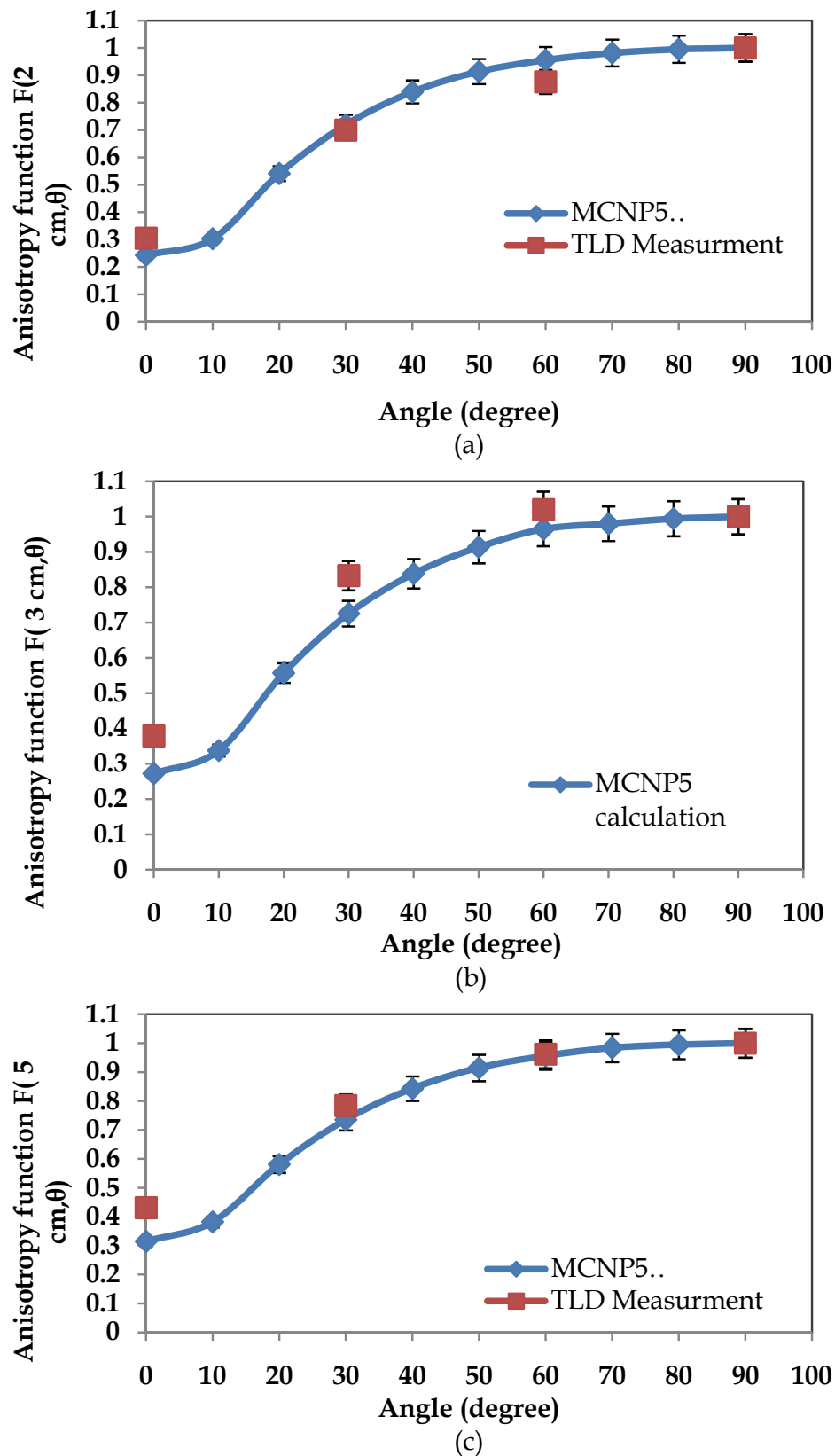


Fig. 4. Comparison between measured (Raisali et al., 2008) and calculated results (Saidi et al., 2010) for IR-<sup>103</sup>Pd seed anisotropy functions at selected radial distances of (a) 2 cm, (b) 3 cm, (c) 5 cm.

(a)  $r^2G(r,\theta)/G(r_0,\theta_0)$  for ideal seed orientation.

r (cm)	0°	10°	20°	30°	40°	50°	60°	70°	80°	90°
0.25	1.529	1.487	1.382	1.260	1.149	1.059	0.992	0.947	0.921	0.912
0.50	1.100	1.098	1.086	1.067	1.046	1.025	1.006	0.992	0.983	0.980
0.75	1.046	1.045	1.041	1.033	1.024	1.015	1.007	1.000	0.996	0.994
1.00	1.025	1.028	1.026	1.021	1.017	1.012	1.007	1.003	1.000	1.000
1.50	1.014	1.016	1.015	1.014	1.011	1.009	1.007	1.005	1.004	1.003
2.00	1.009	1.011	1.011	1.010	1.009	1.008	1.007	1.005	1.005	1.005
3.00	1.001	1.008	1.008	1.008	1.008	1.008	1.007	1.006	1.006	1.006
4.00	1.000	1.008	1.008	1.008	1.007	1.007	1.007	1.006	1.006	1.006
5.00	1.000	1.007	1.007	1.007	1.007	1.007	1.007	1.007	1.006	1.007
7.00	0.998	1.007	1.007	1.007	1.007	1.007	1.007	1.007	1.006	1.006

(b)  $r^2G(r,\theta)/G(r_0,\theta_0)$  for ideal orientation calculated by Raisali et al. (2008)

r (cm)	0°	10°	20°	30°	40°	50°	60°	70°	80°	90°
0.25	1.514	1.484	1.383	1.259	1.148	1.058	0.991	0.947	0.920	0.911
0.50	1.102	1.098	1.086	1.066	1.046	1.025	1.006	0.993	0.983	0.981
0.75	1.068	1.044	1.040	1.033	1.024	1.015	1.007	1.000	0.996	0.994
1.00	1.031	1.028	1.025	1.022	1.017	1.012	1.008	1.003	1.001	1.000
1.50	1.006	1.015	1.014	1.013	1.011	1.009	1.007	1.005	1.004	1.002
2.00	1.002	1.011	1.009	1.010	1.009	1.008	1.007	1.005	1.006	1.005
3.00	0.996	1.008	1.008	1.009	1.007	1.007	1.007	1.007	1.006	1.005
4.00	1.002	1.008	1.008	1.008	1.007	1.006	1.007	1.007	1.006	1.005
5.00	0.997	1.007	1.007	1.007	1.006	1.006	1.006	1.007	1.006	1.007
7.00	0.995	1.008	1.007	1.006	1.006	1.007	1.007	1.007	1.006	1.006

(c)  $r^2G(r,\theta)/G(r_0,\theta_0)$  for vertical seed orientation.

r (cm)	0°	10°	20°	30°	40°	50°	60°	70°	80°	90°	100°	110°	120°	130°	140°	150°	160°	170°	180°
0.25	1.510	1.436	1.275	1.121	0.944	1.529	1.287	1.225	1.086	0.911	0.919	0.930	0.990	1.057	1.102	1.258	1.380	1.452	1.519
0.50	1.915	1.908	1.791	1.650	1.482	1.379	1.230	1.129	1.056	0.980	0.981	0.987	1.006	1.022	1.039	1.067	1.084	1.101	1.088
0.75	1.476	1.460	1.449	1.377	1.317	1.236	1.167	1.106	1.046	0.994	0.994	1.005	1.005	1.015	1.022	1.034	1.039	1.043	1.044
1.00	1.287	1.324	1.297	1.261	1.226	1.177	1.136	1.075	1.035	1.000	0.998	1.002	1.007	1.010	1.018	1.020	1.025	1.034	1.001
1.50	1.164	1.195	1.186	1.169	1.145	1.141	1.091	1.060	1.029	1.003	1.002	1.005	1.007	1.008	1.014	1.012	1.014	1.021	0.987
2.00	1.114	1.147	1.136	1.121	1.107	1.086	1.058	1.045	1.023	1.005	1.003	1.006	1.007	1.008	1.012	1.009	1.009	1.017	0.986
3.00	1.064	1.098	1.082	1.080	1.077	1.114	1.048	1.035	1.019	1.006	1.004	1.006	1.007	1.007	1.011	1.007	1.009	1.014	0.981
4.00	1.039	1.076	1.065	1.061	1.058	1.048	1.065	1.027	1.018	1.006	1.004	1.007	1.007	1.007	1.011	1.006	1.007	1.013	0.979
5.00	1.026	1.063	1.051	1.047	1.052	1.034	1.029	1.026	1.009	1.006	1.004	1.007	1.007	1.008	1.011	1.006	1.006	1.013	0.978
7.00	1.036	1.046	1.045	1.042	1.034	1.027	1.024	1.027	1.010	1.010	1.004	1.011	1.005	1.011	1.011	1.011	1.011	1.002	

(d)  $r^2G(r,\theta)/G(r_0,\theta_0)$  for diagonal seed orientation.

$r$ (cm)	0°	10°	20°	30°	40°	50°	60°	70°	80°	90°	100°	110°	120°	130°	140°	150°	160°	170°	180°
0.25	1.588	1.449	1.324	1.209	1.121	1.027	0.985	0.001	0.909	0.911	0.920	0.929	0.987	1.042	1.097	1.248	1.277	1.435	1.507
0.50	1.020	1.051	1.054	1.046	1.021	1.005	0.994	0.990	0.990	0.980	0.983	0.986	1.004	1.020	1.036	1.062	1.076	1.095	1.073
0.75	0.992	1.001	1.010	1.010	1.000	0.998	0.997	0.994	0.994	1.384	1.388	1.391	1.413	1.432	1.451	1.481	1.498	1.522	1.492
1.00	1.026	0.993	0.993	0.996	0.993	0.996	0.998	0.995	1.000	1.000	1.001	1.002	1.006	1.011	1.016	1.018	1.023	1.031	1.012
1.50	1.012	0.982	0.982	0.984	0.987	0.993	0.998	0.999	1.001	1.004	1.004	1.004	1.006	1.009	1.013	1.011	1.015	1.020	1.002
2.00	0.996	0.977	0.979	0.982	0.984	0.990	0.996	1.002	1.001	1.005	1.005	1.006	1.006	1.009	1.012	1.008	1.012	1.017	0.992
3.00	0.989	0.975	0.977	0.986	0.985	0.992	0.999	1.003	1.002	1.006	1.006	1.007	1.006	1.009	1.011	1.006	1.012	1.014	0.987
4.00	0.998	0.975	0.978	0.989	0.989	0.995	1.002	1.003	1.003	1.007	1.007	1.007	1.007	1.009	1.011	1.006	1.012	1.014	0.983
5.00	1.005	0.985	0.979	0.990	0.992	1.001	1.007	1.007	1.004	1.007	1.007	1.007	1.007	1.009	1.011	1.005	1.007	1.013	0.982
7.00	1.003	0.985	0.978	0.990	0.992	1.001	1.007	1.007	1.004	1.225	1.225	1.225	1.231	1.231	1.219	1.225	1.237	1.175	

Table 3. Monte Carlo calculated  $r^2G(r,\theta)/G(r_0,\theta_0)$  for the IR- $^{103}\text{Pd}$  seed (Saidi et al., 2010) in (a) ideal orientation , (b) ideal orientation calculated by Raisali et al. (2008), (c) vertical orientation, (d) diagonal orientation.

Also in this example authors benchmarked their MCNP simulation with the new  $^{103}\text{Pd}$  source (Rivard et al., 2004b) to demonstrate the accuracy of their simulation. For the three seed orientations, the values of  $\Lambda$  in three orientations, ranged from 0.716 to 0.753 cGyU-1h-1, with the geometry uncertainty of 1.5% for this seed. According to TG43U1, a standard uncertainty of 3% for all Monte Carlo studies seems reasonable. Authors claimed that the difference between the calculated values of dose rate constant by the Raisali et al., (2008) value, derives from the use of different methods to calculate the air-kerma strength,  $S_K$ . Raisali et al. calculated  $S_K$  only in one air-filled detector placed at a distance of one meter in the transverse plane of the seed. Also use of two different versions of MCNP code, MCNP4C & MCNP5 with two different cross section libraries and two different simulation geometries cause such a difference in the obtained values. Table 2 shows the calculated dose rate constant for the IR- $^{103}\text{Pd}$  seed (Saidi et al., 2010), new  $^{103}\text{Pd}$  source (Rivard et al., 2004b) and the calculated and measured values of  $\Lambda$ , for NASI model MED3633 and Theragenics model 200 sources (Rivard et al., 2004b).

The Monte Carlo calculated values of geometry function in this example for three orientations are shown in Table 3(a), (c) and (d). They used the form,  $r^2G(r,\theta)$ , instead of  $G(r,\theta)$ , for easier calculations and then normalized to  $G(1\text{cm}, \pi/2)$  for convenience to compare with other published data (Rivard, 2001; King et al., 2001). The results were compared with Raisali et al., (2008) data.

The calculated line and point source radial dose function for the ideal orientation of the IR- $^{103}\text{Pd}$  seed in Perspex and water in this example and those determined from calculated and measurement by (Raisali et al., 2008) are presented in Table 4. Figure 3 shows a comparison of the radial dose function of IR- $^{103}\text{Pd}$  seed with MED3633 and Theragenics model 200 sources.

As TG43-U1 recommendation,  $g_L(r)$  for ideal orientation in water was fit to a fifth order polynomial function (Equation 8):

Where  $a_0 = 1.534$ ,  $a_1 = -5.933 \times 10^{-1}$ ,  $a_2 = 2.731 \times 10^{-2}$ ,  $a_3 = 2.362 \times 10^{-2}$ ,  $a_4 = -4.778 \times 10^{-3}$  and  $a_5 = 2.783 \times 10^{-4}$  define  $R^2 = 9.998 \times 10^{-1}$ .

r (cm)	$g_L(r)$ (Perspex)			$g_L(r)$ (Water)		$g_P(r)$ (Water)
	MCNP5 Saidi et al. (2010)	TLD Raisali et al. (2008)	MCNP4C Raisali et al. (2008)	MCNP5 Saidi et al. (2010)	MCNP4C Raisali et al. (2008)	MCNP5 Saidi et al. (2010)
0.25	1.532	-	1.168	1.390	1.339	1.092
0.5	1.242	1.15	1.134	1.242	1.239	1.229
0.75	1.077	-	1.070	1.112	1.119	1.114
1	1.000	1.00	1.000	1.000	1.000	1.000
1.5	0.711	0.82	0.849	0.763	0.783	0.773
2	0.668	0.78	0.706	0.573	0.602	0.573
3	0.393	0.51	0.473	0.331	0.348	0.334
4	0.169	0.31	0.306	0.165	0.198	0.166
5	0.085	0.20	0.195	0.089	0.111	0.090
7	0.025	-	-	0.027	0.035	0.027

Table 4. Monte Carlo calculations for radial dose function,  $g_L(r)$  and  $g_P(r)$  for line and point source geometry for IR- $^{103}\text{Pd}$  seed with an effective length of 0.3 mm, in comparison with TLD measurements of Raisali et al., (2008) in Perspex and also calculated in water.

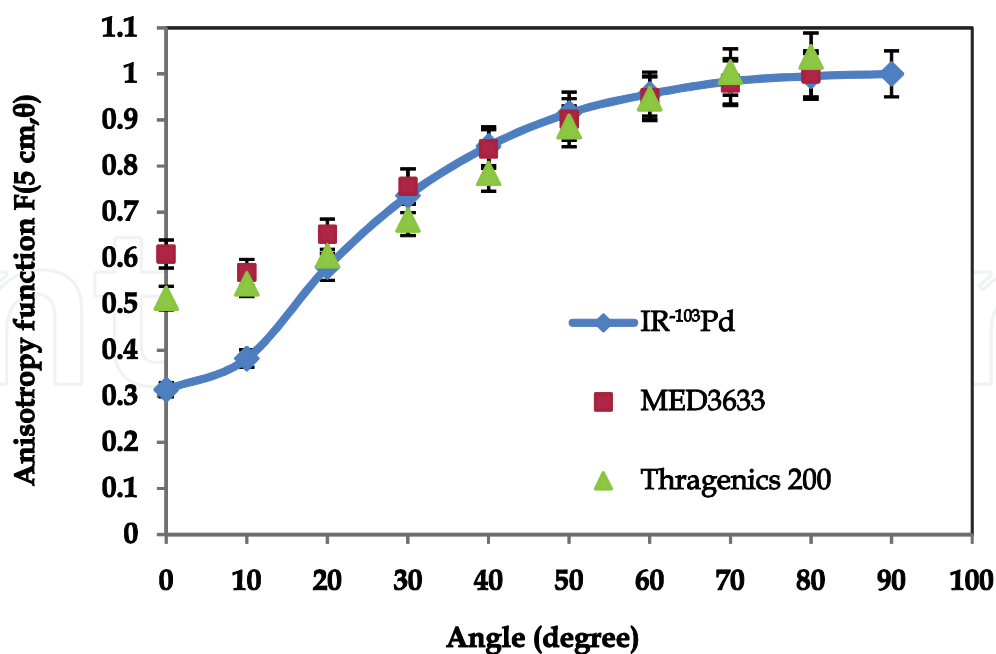


Fig. 5. Comparison of the Monte Carlo calculation anisotropy function of IR- $^{103}\text{Pd}$  seed (Saidi et al., 2010) with the MED3633 and Theragenics model 200 sources (Rivard et al., 2004a) at the distance of 5 cm.

The anisotropy function,  $F(r,\theta)$ , of the IR- $^{103}\text{Pd}$  seed was calculated in Perspex phantom at radial distances of  $r = 0.25, 0.5, 0.75, 1, 1.5, 2, 3, 4, 5$  and  $7\text{ cm}$  relative to the seed center and polar angle,  $\theta$  ranging from  $0^\circ$  to  $90^\circ$  for ideal orientation and  $0^\circ$  to  $180^\circ$  for vertical and diagonal orientations in  $10^\circ$  increment with respect to the seed long axis. Saidi et al.'s (2010) results are shown in Table 5 and compared with the measured data by Raisali et al., (2010), for ideal orientation. The data are shown graphically at distances of 2, 3 and 5 cm in Figure 4. Figure 5 shows a comparison of the anisotropy function at  $r = 5\text{ cm}$  of the IR- $^{103}\text{Pd}$  with MED3633 and Theragenics model 200 sources.

## 10. Acknowledgements

"Research supported by WCU program through NRF Korea funded by MEST (R31-2008-000-10029-0)"

(a) 2D anisotropy function,  $F(r,\theta)$  in ideal seed orientation

$r\text{ (cm)}$	$0^\circ$	$10^\circ$	$20^\circ$	$30^\circ$	$40^\circ$	$50^\circ$	$60^\circ$	$70^\circ$	$80^\circ$	$90^\circ$	$\Phi_{an}(r)$
0.25	0.025	0.076	0.656	0.833	0.906	0.950	0.975	0.991	0.998	1.000	1.023
0.50	0.106	0.162	0.505	0.738	0.864	0.926	0.962	0.985	0.996	1.000	0.910
0.75	0.150	0.206	0.505	0.720	0.851	0.921	0.959	0.984	0.996	1.000	0.892
1.00	0.158	0.221	0.482	0.674	0.794	0.862	0.901	0.924	0.936	1.000	0.838
1.50	0.206	0.276	0.529	0.717	0.841	0.915	0.956	0.982	0.995	1.000	0.861
2.00	0.243	0.303	0.541	0.720	0.840	0.914	0.956	0.982	0.995	1.000	0.884
3.00	0.272	0.338	0.557	0.726	0.839	0.914	0.955	0.980	0.994	1.000	0.885
4.00	0.298	0.362	0.571	0.731	0.842	0.912	0.955	0.981	0.995	1.000	0.887
5.00	0.314	0.382	0.581	0.735	0.843	0.915	0.956	0.984	0.995	1.000	0.889
7.00	0.377	0.417	0.610	0.747	0.848	0.916	0.951	0.979	1.000	1.000	0.894

(b) 2D anisotropy function,  $F(r,\theta)$  in vertical seed orientation

$r\text{ (cm)}$	$0^\circ$	$10^\circ$	$20^\circ$	$30^\circ$	$40^\circ$	$50^\circ$	$60^\circ$	$70^\circ$	$80^\circ$	$90^\circ$	$100^\circ$	$110^\circ$	$120^\circ$	$130^\circ$	$140^\circ$	$150^\circ$	$160^\circ$	$170^\circ$	$180^\circ$
0.250	0.039	0.487	0.671	0.862	0.966	0.928	0.993	0.989	0.996	1.000	0.807	0.802	0.783	0.778	0.739	0.658	0.459	0.326	0.024
0.500	0.157	0.380	0.528	0.771	0.900	0.953	0.967	0.988	0.979	1.000	0.801	0.814	0.787	0.759	0.731	0.605	0.394	0.283	0.112
0.750	0.217	0.425	0.303	0.748	0.865	0.887	0.917	0.979	0.999	1.000	0.828	0.814	0.756	0.723	0.709	0.598	0.231	0.321	0.180
1.000	0.173	0.354	0.455	0.608	0.732	0.790	0.777	0.801	0.810	1.000	0.809	0.803	0.774	0.782	0.716	0.587	0.422	0.325	0.184
1.500	0.271	0.468	0.639	0.757	0.898	0.931	0.962	0.987	0.993	1.000	0.993	0.990	0.957	0.935	0.883	0.730	0.597	0.437	0.274
2.000	0.308	0.492	0.630	0.762	0.893	0.983	0.962	0.989	0.994	1.000	0.957	0.990	0.957	1.033	0.883	0.735	0.593	0.462	0.307
3.000	0.359	0.523	0.603	0.769	0.898	0.933	0.961	0.989	0.998	1.000	0.997	0.989	0.956	0.927	0.882	0.743	0.568	0.493	0.352
4.000	0.384	0.549	0.704	0.784	0.902	0.931	0.963	0.995	0.999	1.000	0.998	0.990	0.958	0.917	0.883	0.752	0.666	0.514	0.370
5.000	0.422	0.567	0.674	0.782	0.913	0.907	0.961	0.996	0.998	1.000	0.997	0.987	0.955	1.000	0.883	0.756	0.638	0.531	0.398
7.000	0.398	0.408	0.597	0.739	0.873	0.919	0.949	0.996	0.999	1.000	0.998	0.979	0.999	0.900	0.848	0.993	0.999	0.997	0.427

(c) 2D anisotropy function,  $F(r,\theta)$  in diagonal seed orientation

r (cm)	0°	10°	20°	30°	40°	50°	60°	70°	80°	90°	100°	110°	120°	130°	140°	150°	160°	170°	180°
0.250	0.026	0.075	0.630	0.801	0.887	0.924	0.970	0.985	0.988	1.000	1.000	1.000	1.000	0.997	0.995	0.995	1.033	0.974	0.974
0.500	0.098	0.170	0.492	0.725	0.846	0.909	0.953	0.985	1.005	1.000	1.000	1.000	1.000	0.997	0.995	0.995	0.986	0.974	0.974
0.750	0.139	0.220	0.490	0.706	0.833	0.906	0.950	0.982	1.002	1.000	1.000	1.000	1.000	0.997	0.995	0.995	0.986	0.974	0.974
1.000	0.223	0.342	0.659	0.927	1.095	1.198	1.260	1.294	1.321	1.000	1.409	1.409	1.409	1.405	1.401	1.401	1.388	1.372	1.372
1.500	0.206	0.292	0.513	0.699	0.822	0.902	0.949	0.978	0.995	1.000	1.000	1.000	1.000	0.997	0.995	0.995	0.985	0.974	0.974
2.000	0.240	0.312	0.525	0.701	0.821	0.900	0.948	0.981	0.993	1.000	1.000	1.000	1.000	0.997	0.995	0.995	0.985	0.974	0.974
3.000	0.270	0.353	0.541	0.709	0.822	0.905	0.950	0.979	0.992	1.000	1.000	1.000	1.000	0.997	0.995	0.995	0.982	0.974	0.974
4.000	0.296	0.383	0.555	0.716	0.829	0.906	0.955	0.981	0.994	1.000	1.000	1.000	1.000	0.997	0.995	0.995	0.982	0.974	0.974
5.000	0.317	0.410	0.566	0.725	0.832	0.911	0.958	0.986	0.995	1.000	1.000	1.000	1.000	0.997	0.995	0.995	0.986	0.974	0.974
7.000	0.380	0.448	0.594	0.736	0.837	0.913	0.953	0.981	1.000	1.000	1.000	1.000	1.000	0.995	0.986	0.987	0.885	0.867	0.876

Table 5. 2D anisotropy functions for the IR-<sup>103</sup>Pd seed calculated by Monte Carlo method (Saidi et al., 2010) for the (a) ideal orientation, (b) vertical orientation, (c) diagonal orientation.

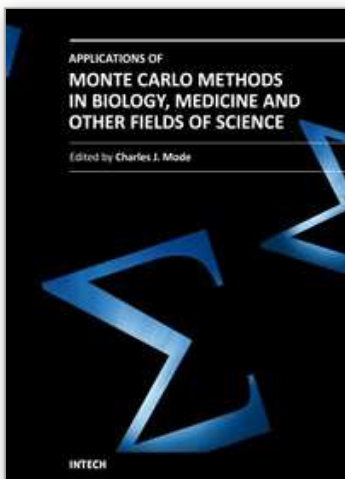
## 11. References

- Anagnostopoulos, G.; Baltas, D.; Karaiskos, P.; Pantelis, E.; Papagiannis, P. & Sakellou, L. (2003). An analytical dosimetry model as a step towards accounting for inhomogeneities and bounded geometries in <sup>192</sup>Ir brachytherapy treatment planning. *Phys. Med. Biol.*, 48, 11, (May 2003), 1625-1634, ISSN: 1361-6560.
- Antipas, V.; Dale, R.G. & Coles, I.P. (2001). A theoretical investigation into the role of tumour radiosensitivity, clonogen repopulation, tumour shrinkage and radionuclide RBE in permanent brachytherapy implants of <sup>125</sup>I and <sup>103</sup>Pd. *Phys Med Biol.* 46, 10, (September 2001), 2557-2569, ISSN: 1361-6560.
- Ataeinia, V.; Raisali, Gh.; Sadeghi, M. (2009). Determination of dosimetry parameters of ADVANTAGETM 103Pd brachytherapy seed using MCNP4C computer code. *NUKLEONIKA*. 54, 3, (May 2009), 181-187, ISSN: 0029-5922.
- Baltas, D.; Karaiskos, P.; Papagiannis, P.; Sakellou, L.; Loeffler, E. & Zamboglou, N. (2001). Beta versus gamma dosimetry close to Ir-192 brachytherapy sources, *Med. Phys.* 28, 9, (June 2001), 1875-1882, ISSN: 0094-2405.
- Baltas, D.; Sakellou, L. & Zamboglou, N. (2007). *The Physics of Modern Brachytherapy for Oncology*. Taylor & Francis, ISBN-13: 978-0-7503-0708-6, London-New York.
- Baltimore, M.D. (1995). Collaborative Ocular Melanoma Medium Tumor Trial, Manual of procedure. COMS Coordinating centre.
- Chibani, O.; Williamson, J.F. & Todor, D. (2005). Dosimetric effects of seed anisotropy and interseed attenuation for <sup>103</sup>Pd and <sup>125</sup>I prostate implants. *Med. Phys.* 32, 8, (July 2005), 2557-2566, ISSN: 0094-2405.
- Chiu-Tsao, S.; Anderson, L.L.; O'Brien, K.; Stabile, L. & Liu, J.C. (1993). Dosimetry for <sup>125</sup>I seed (model 6711) in eye plaque. *Med. Phys.* 20, 2, (November 1992), 383-389, ISSN: 0094-2405.
- Chiu-Tsao, S.T.; Schaart, D.R. & Nath, R. (2007). Dose calculation formalism and consensus dosimetry parameters for intravascular brachytherapy dosimetry:

- Recommendations of the AAPM Therapy Physics Committee Task Group No. 149. *Med Phys.* 34, 11, (October 2007), 4126-4157, ISSN: 0094-2405.
- Cross section Evaluation Working Group, ENDF/B-VI Summary documentation (ENDF-201), Brookhaven National Laboratory Report No. BNL.NCS-17541, 8th ed., 2000. National Nuclear Data Centre.
- Dale, R.G. (1982). A Monte Carlo derivation of parameters for use in the tissue dosimetry of medium and low energy nuclides. *Br. J. Radiol.* 55, 658, (October 1982), 748-757, ISSN: 1748-880X.
- Devic, S.; Monroe, J.I.; Mutic, S.; Whiting, B. & Williamson, J.F. (2000). Dual Energy CT Tissue Quantitation for Monte-Carlo Based Treatment Planning for Brachytherapy 1-MO E309-01 (Chicago, IL: IEEE Engineering Medicine and Biology Society).
- Finger, P.T.; Moshfeghi, D.M. & Ho, T.K. (1991). Palladium-103 ophthalmic plaque radiotherapy. *Arch Ophthalmol.* 109, 11, (July 1991), 1610-1613, ISSN: 0003-9950.
- Finger, P.T.; Berson, A. & Szechter, A. (1999). Palladium-103 plaque radiotherapy for choroidal melanoma: results of a 7year study. *Ophthalmology.* 106, 3, (March 1999), 606-613, ISSN: 1549-4713.
- Gearheart, D.; Drogin, A.; Sowards, K.; Meigooni, A.S. & Ibbott, G.S. (2000). Dosimetric characteristics of a new <sup>125</sup>I brachytherapy source. *Med. Phys.* 27, 10, (October 2000), 2278-2285, ISSN: 0094-2405.
- Granero, D.; Perez-Calatayud, J.; Ballester, F. & Casal, E. (2004). Dosimetric study of the 15 mm Ropes eye plaque. *Med.Phys.* 31, 12, (December 2004), 3330-3336, ISSN: 0094-2405.
- Hall, E.J. & Brenner, D.J. (1991). The dose rate effect revisited: radiobiological considerations of importance in radiotherapy. *Int J Radiat Oncol Biol Phys.* 21, 6, (November 1991), 1403-1414, ISSN: 0360-3016.
- Hosseini, S.H.; Sadeghi, M. & Ataeinia, V. (2009). Dosimetric comparison of four new design <sup>103</sup>Pd brachytherapy sources: Optimal design using silver and copper rod cores, *Med. Phys.* 36, 7, (July 2009), 3080-3085, ISSN: 0094-2405.
- Huang, D.Y.C.; Schell, M.C.; Weaver, K.A. & Ling, C.C. (1990). Dose distribution of <sup>125</sup>I sources in different tissues. *Med. Phys.* 17, 5, (September 1990), 826-832, ISSN: 0094-2405.
- ICRU, International Commission on Radiation Units and Measurements, (1985). Dose and volume specification for reporting intracavitary therapy in gynecology, *ICRU Report 38.*
- Karaiskos, P.; Sakelou, L.; Sandilos, P. & Vlachos, L. (2000). Limitations of the point and line source approximations for the determination of geometry factors around brachytherapy sources. *Med. Phys.* 27, 1, (January, 2000), 124-128, ISSN: 0094-2405.
- King, P.P.; Anderson, R.S. & Mills, M.D. (2001). Geometry function of a linear brachytherapy source. *J. Appl. Clin. Med. Phys.* 2, 2, (April 2001), 69-72, ISSN: 1526-9914.
- Levitt, S.H.; Purdy, J.A.; Perez, Vijayakumar, C.A.S. (2006). *Technical Basis of Radiation Therapy.* Practical Clinical Applications. Springer, ISBN-10 3-540-21338-4 Berlin Heidelberg New York.
- Li, Z.; Palta, J.R. & Fan, J.J. (2000). Monte Carlo calculations and experimental measurements of dosimetry parameters of a new <sup>103</sup>Pd source. *Med. Phys.* 27, 5, (May 2000), 1108-1112, ISSN: 0094-2405.
- Ling, C.C.; Li, W.X. & Anderson, L.L. (1995). The relative biological effectiveness of I-125 and Pd-103. *Int J Radiat Oncol Biol Phys.* 32, 2, (May 1995), 373-378, ISSN: 0360-3016.
- Mayles, Ph.; Nahum, A.E. & Rosenwald, J.C. (2007). *Hand book of radiotherapy physics: theory and practice.* Taylor & Francis, ISBN-13: 978-0-7503-0860-1, New York London.

- Melhus, C.S. & Rivard, M.J. (2006). Approaches to calculating AAPM TG-43 brachytherapy dosimetry parameters for  $^{137}\text{Cs}$ ,  $^{125}\text{I}$ ,  $^{192}\text{Ir}$ ,  $^{103}\text{Pd}$  and  $^{169}\text{Yb}$  sources. *Med. Phys.* 33, 6, (June 2006), 1729-1737, ISSN: 0094-2405.
- Melhus, C.S. & Rivard, M.J. (2008). COMS eye plaque brachytherapy dosimetry simulations for  $^{103}\text{Pd}$ ,  $^{125}\text{I}$ , and  $^{131}\text{Cs}$ . *Med. Phys.* 35, 7, (July 2008), 3364-3371, ISSN: 0094-2405.
- Melia, B.M.; Abramson, D.H.; Albert, D.M.; Boldt, H.C.; Earle, J.D.; Hanson, W.F.; Montague, P.; Moy, C.S.; Schachat, A.P.; Simpson, E.R.; Straatsma, B.R.; Vine, A.K.; Weingeist, T.A. & Collaborative Ocular Melanoma Study Group. (2001). Collaborative Ocular Melanoma Study (COMS) randomized trial of I-125 brachytherapy for medium choroidal melanoma. I. Visual acuity after 3 years. COMS report no. 16. *Ophthalmology*. 108, 2, (February 2001), 348-366, ISSN: 0003-9950.
- Monte Carlo Team, MCNP-A General Monte Carlo N-Particle Transport Code-Version 5, Los Alamos National Laboratory, <http://mcnp-green.lanl.gov/index.html>, (last reviewed 29-Jan-2004).
- Nag, S.; Quivey, J.; Earle, J.; Followill, D.; James Fontanesi J.; Finger, P.T.; F.A.C.S. & American Brachytherapy Society. (2003). The American Brachytherapy Society recommendations for brachytherapy of uveal melanomas. *Int J Radiat Oncol Biol Phys.* 56, 2, (June 2003), 544-555, ISSN: 0360-3016.
- Nath, R.; Anderson, L.L.; Luxton, G.; Weaver, K.A.; Williamson, J.F. & Meigooni, A.S. (1995). Dosimetry of interstitial brachytherapy sources: Recommendations of the AAPM Radiation Therapy Committee Task Group No. 43. *Med. Phys.* 22, 2, (February 1995), 209-234, ISSN: 0094-2405.
- Nath, R.; Anderson, L.L.; Meli, J.A.; Olch, A.J.; Stitt, J.A. & Williamson, J.F. (1997). Code of practice for brachytherapy physics: Report of the AAPM Radiation Therapy Committee Task Group No. 56. *Med. Phys.* 24, 10, (October 1997), 1557-1998, ISSN: 0094-2405.
- Nath, R.; Bongiorni, P.; Chen, Z.; Gragnano, J. & Rockwell, S. (2005). Relative biological effectiveness of  $^{103}\text{Pd}$  and  $^{125}\text{I}$  photons for continuous low-dose-rate irradiation of Chinese hamster cells. *Radiat Res.* 163, 5, (May 2005), 501-509.
- Nath, R.; Yue, N.; Shahnazi, K. & Bongiorni, P.J. (2000). Measurement of dose-rate constant for  $^{103}\text{Pd}$  seeds with air kerma strength calibration based upon a primary national standard. *Med. Phys.* 27, 4, (April 2000), 655-658, ISSN: 0094-2405.
- Perez-Catalayud, J.; Granero, D. & Ballester, F. (2004). Phantom size in brachytherapy source dosimetric studies. *Med. Phys.* 31, 7, (July 2004), 2075-2081, ISSN: 0094-2405.
- Perez-Calatayud, J.; Granero, D.; Ballester, F. (2009). *Monte Carlo Application in Brachytherapy Dosimetry*, In: *Radiotherapy and Brachytherapy*, Lemoigne, Y. & Caner, A. (Ed.), 239-250, Springer, ISBN: 978-90-481-3096-2, France.
- Prasad, S.C. & Bassano, D.A. (1985). Lung density effect on  $^{125}\text{I}$  distribution. *Med. Phys.* 12, 1, (January 1985), 99-100, ISSN: 0094-2405.
- Raisali, Gh.; Sadeghi, M.; Ataenia, V.; Shahvar, A. & Ghonchehnazi, M. (2008). Determination of Dosimetric Parameters of the Second Model of Pd-103 Seed Manufactured at Agricultural, Medical and Industrial Research School. *Iranian J. Med. Phys.* 5, 1, (July 2008), 9-20. (Persian)
- Rivard, M.J. (2001). Monte Carlo calculation of AAPM Task Group Report No.43 dosimetry parameters for the MED3631-A/M  $^{125}\text{I}$  source. *Med. Phys.* 28, 4, (April 2001), 629-637. ISSN: 0094-2405.
- Rivard, M.J.; Coursey, B.M.; DeWerd, L.A.; Hanson, W.F.; Huq, M.S.; Ibbott, G.S.; Mitch, M.G.; Nath, R. & Williamson, J.F. (2004a). "Update of AAPM Task Group No. 43 Report: A revised AAPM protocol for brachytherapy dose calculations. *Med. Phys.* 31, 3, (March 2004), 633-674, ISSN: 0094-2405.

- Rivard, M.J.; Melhus, C.S. & Kirk, B.L. (2004b). Brachytherapy dosimetry parameters calculated for a new  $^{103}\text{Pd}$  source. *Med. Phys.* 31, 9, (September 2004), 2466-2470, ISSN: 0094-2405.
- Rivard, M.J. (2007). Brachytherapy dosimetry parameters calculated for a  $^{137}\text{Cs}$ . *Med. Phys.* 34, 2, (February 2007) 754-762, ISSN: 0094-2405.
- Rogers D. W. O. (2006). Fifty years of Monte Carlo simulations for medical physics. *Phys. Med. Biol.* 51, 13, (June 2006), R287-R301.
- Sadeghi, M.; Raisali, Gh.; Hosseini, S.H.; Shahvar, A. (2008a), Monte Carlo calculations and experimental measurements of dosimetric parameters of the IRA- $^{103}\text{Pd}$  brachytherapy source. *Med. Phys.* 35, 4, (April 2008), 1288-1294, ISSN: 0094-2405.
- Sadeghi, M.; Hosseini, S.H.; Raisali, Gh. (2008b). Experimental measurements and Monte Carlo calculations of dosimetric parameters of the IRA1- $^{103}\text{Pd}$  brachytherapy source. *Appl. Radiat. Isot.* 66, 10, (October 2008), 1431-1437, ISSN: 0969-8043.
- Sadeghi, M.; Karimi, E.; Hosseini, S.H. (2009a). Dosimetric comparison of  $^{90}\text{Y}$ ,  $^{32}\text{P}$ , and  $^{186}\text{Re}$  radiocolloids in craniopharyngioma treatments. *Med. Phys.* 36, 11, (November 2009), 5022-5026. ISSN: 0094-2405.
- Sadeghi, M.; Hosseini, S.H. (2010). Study of the IsoAid ADVANTAGETM  $^{125}\text{I}$  brachytherapy source dosimetric parameters using Monte Carlo simulation. *Appl. Radiat. Isot.* 68, 1, (January 2010), 211-213, ISSN: 0969-8043.
- Saidi, P. M. Sadeghi, M, Shirazi, A. & Tenreiro, C. (2010). Monte Carlo calculation of dosimetry parameters for the IR08- $^{103}\text{Pd}$  brachytherapy source. *Med. Phys.* 37, 6, (June 2010), 2509-2515. ISSN: 0094-2405.
- Thomson, R.M.; Taylor, R.E.P. & Rogers, D.W.O. (2008). Monte Carlo dosimetry for  $^{125}\text{I}$  and  $^{103}\text{Pd}$  eye plaque brachytherapy. *Med.Phys.* 35, 12, (December 2008), 5530-5543, ISSN: 0094-2405.
- Thomson, R.M. & Rogers D.W.O. (2010) Monte Carlo dosimetry for  $^{125}\text{I}$  and  $^{103}\text{Pd}$  eye plaque brachytherapy with various seed model. *Med. Phys.* 37, 1, (January 2010), 368-376, ISSN: 0094-2405.
- Wallace, R.E. & Fan, J.J. (1999). Dosimetric characterization of a new design 103palladium brachytherapy source. *Med. Phys.* 26, 11, (November 1999) 2465-2470, ISSN: 0094-2405.
- Wang, R. & Li, X.A. (2000).A Monte Carlo calculation of dosimetric parameters of  $^{90}\text{Sr}/^{90}\text{Y}$  and  $^{192}\text{Ir}$  SS sources for intravascular brachytherapy. *Med. Phys.* 27, 11, (November 1999), 2528, 2000. ISSN: 0094-2405.
- Williamson, J.F. (1991). Comparison of measured and calculated dose rates in water near I-125 and Ir-192 seeds. *Med. Phys.* 18, 4, (July 1991), 776-786, ISSN: 0094-2405.
- Williamson, J.F.; Coursey, B.M.; DeWerd, L.A.; Hanson, W.F.; Nath, R.; Rivard, M.J. & Ibbott, G. (1999). On the use of apparent activity ( $A_{app}$ ) for treatment planning of  $^{125}\text{I}$  and  $^{103}\text{Pd}$  interstitial sources: Recommendations of the American Association of Physicists in Medicine Radiation Therapy Committee Subcommittee on Low-Energy Brachytherapy Source Dosimetry, *Med. Phys.* 26,12, (December 1999), 2529 - 2530, ISSN: 0094-2405.
- Williamson, J.F. (2000). Monte Carlo modelling of the transverse-axis dose distribution of the model 200  $^{103}\text{Pd}$  interstitial brachytherapy source. *Med. Phys.* 27, 4, (April 2000), 643-654. ISSN: 0094-2405.
- Williamson, J.F. (2006). Brachytherapy technology and physics practice since 1950: a half-century of progress. *Phys. Med. Biol.* 51, 13, (June 2006), R303-R325, ISSN: 1361-6560.
- Wuu, C.S. & Zaider, M. (1998). A calculation of the relative biological effectiveness of  $^{125}\text{I}$  and  $^{103}\text{Pd}$  brachytherapy sources using the concept of proximity function. *Med Phys.* 25, 11, (November 1998), 2186-2189. ISSN: 0094-2405.



## **Applications of Monte Carlo Methods in Biology, Medicine and**

### **Other Fields of Science**

Edited by Prof. Charles J. Mode

ISBN 978-953-307-427-6

Hard cover, 424 pages

**Publisher** InTech

**Published online** 28, February, 2011

**Published in print edition** February, 2011

This volume is an eclectic mix of applications of Monte Carlo methods in many fields of research should not be surprising, because of the ubiquitous use of these methods in many fields of human endeavor. In an attempt to focus attention on a manageable set of applications, the main thrust of this book is to emphasize applications of Monte Carlo simulation methods in biology and medicine.

### **How to reference**

In order to correctly reference this scholarly work, feel free to copy and paste the following:

Mahdi Sadeghi, Pooneh Saidi and Claudio Tenreiro (2011). Dosimetric Characteristics of the Brachytherapy Sources Based on Monte Carlo Method, Applications of Monte Carlo Methods in Biology, Medicine and Other Fields of Science, Prof. Charles J. Mode (Ed.), ISBN: 978-953-307-427-6, InTech, Available from: <http://www.intechopen.com/books/applications-of-monte-carlo-methods-in-biology-medicine-and-other-fields-of-science/dosimetric-characteristics-of-the-brachytherapy-sources-based-on-monte-carlo-method>



#### **InTech Europe**

University Campus STeP Ri  
Slavka Krautzeka 83/A  
51000 Rijeka, Croatia  
Phone: +385 (51) 770 447  
Fax: +385 (51) 686 166  
[www.intechopen.com](http://www.intechopen.com)

#### **InTech China**

Unit 405, Office Block, Hotel Equatorial Shanghai  
No.65, Yan An Road (West), Shanghai, 200040, China  
中国上海市延安西路65号上海国际贵都大饭店办公楼405单元  
Phone: +86-21-62489820  
Fax: +86-21-62489821

© 2011 The Author(s). Licensee IntechOpen. This chapter is distributed under the terms of the [Creative Commons Attribution-NonCommercial-ShareAlike-3.0 License](#), which permits use, distribution and reproduction for non-commercial purposes, provided the original is properly cited and derivative works building on this content are distributed under the same license.

IntechOpen

IntechOpen